



1 **Comparing water uptake patterns of two plantations using stable isotopes in Chinese Loess**

2 **Plateau**

3 Yongsheng Cui^a, Chengzhong Pan^{*}, Lan Ma^{b,c}, Zhanwei Sun^b

4
5 *a, College of Water Sciences, Beijing Normal University, Beijing 100875, PR China*

6 *b, Key laboratory of State Forestry Administration on Soil and Water Conservation, School of Soil and Water*
7 *Conservation, Beijing Forestry University, Beijing 100083, PR China*

8 *c, Jixian National Forest Ecosystem Observation and Research Station, CNERN, School of Soil and Water*
9 *Conservation, Beijing Forestry University, Beijing 100083, PR China*

10

11 Number of text pages: 27

12 Number of tables: 2

13 Number of figures: 6

14

15 **Running title: water uptake modes of two plantations**

16

17

18 * Correspondence to:

19 Dr. Chengzhong Pan

20 College of Water Sciences, Beijing Normal University

21 Xijiekouwai Street 19, Beijing 100875, P.R. China;

22 Tel: ++86-10-58802736

23 Fax: ++86-10-58802739

24 E-mail: pancz@bnu.edu.cn

25

26

27



28 Abstract

29 Understanding the water consumption mechanism of plantations is of great significance for the selection of
30 afforestation trees and ecologically sustainable watershed management in semi-arid areas. In this study, *Robinia*
31 *pseudoacacia* and *Pinus tabulaeformis* plantations, which have been widely planted in Chinese Loess Plateau, were
32 selected to investigate the possible difference in water uptake modes. The spatial and temporal variations in
33 precipitation, xylem and soil water stable isotope compositions ($\delta^2\text{H}$, $\delta^{18}\text{O}$) in 2019–2020 were analyzed, and the
34 water uptake modes of plantations were quantified using the direct inference approach and MixSIAR model, with
35 contrasting soil moisture dynamics. The results showed that $\delta^{18}\text{O}$ values were positively correlated with air
36 temperature and negatively correlated with precipitation volume. The $\delta^{18}\text{O}$ content of surface soil (0–40 cm) closely
37 related precipitation input, while those of deep soil layers (100–200 cm) remained stable. When compared with the
38 direct inference approach, the MixSIAR model performed more effectively in quantifying water apportionment,
39 especially in a drought year. In a drought year, *R. pseudoacacia* showed strong drought resilience to absorb water
40 from deep soil, the soil layers of 0–40 cm and 40–200 cm contributed 32.9% and 67.1% to water absorption of *R.*
41 *pseudoacacia*, and 62.2% and 37.8% to that of *P. tabulaeformis*, respectively, while there appeared to be minor
42 differences in soil water uptake between the two plantations in a humid year. Generally, *R. pseudoacacia* consumed
43 more water than *P. tabulaeformis*, especially in a humid year, and the former inclined to absorb soil layer with
44 enriched soil moisture. The results indicated that *R. pseudoacacia* plantation may increase transpiration and cause
45 dried deep soil layers when compared with *P. tabulaeformis*. This study improves our understanding of water uptake
46 mechanisms of plantations and helps with selection of suitable plant species for ecological management in Chinese
47 Loess Plateau.

48 Keywords

49 Root water uptake; Stable isotope; Soil water storage; Plantation; MixSIAR model

50 1. Introduction



51 Soil moisture is the main water source of vegetation growth, especially for the Loess Plateau in China with
52 deep soil layers. It has been proved that large-scale afforestation programs since the 1990s, especially plantations,
53 could increase transpiration and soil water consumption, leading to increased potential for soil desiccation (Liu et
54 al., 2018; Jia et al., 2017; Ma et al., 2014). Therefore, it is urgent and necessary to identify a reasonable vegetation
55 restoration scheme to protect the fragile ecosystems in the Loess Plateau.

56 Plants absorb soil water through root systems and transport it to stem and leaves, where it then dissipates into
57 the atmosphere. Traditionally, the variation in soil water content (SWC) in different soil layers was measured to
58 estimate plant water utilization, and the dynamics of soil water storage helps us to understand the relationship
59 between root water uptake (RWU) and soil moisture (Qiu et al., 2021; Fang et al., 2016; Jackisch et al., 2020). The
60 soil layers of 0–200 cm was classified as an active layers based on the temporal change in SWC (Wang et al., 2015).
61 However, this method cannot accurately depict all water sources and is restricted by the labor-intensive nature of
62 these measurements.

63 The stable isotopic technique shed light on the study of plant water uptake patterns. As the “fingerprint of water”
64 (Meißner et al., 2013), the natural stable isotopes of hydrogen and oxygen in water serve as important recorders of
65 hydrological and ecological processes, providing solid information to explore the water transformation between
66 different water pools, e.g., atmosphere, soil and plant (West et al., 2006; Dai et al., 2020; Barnes and Allison, 1988;
67 Mahindawansa et al., 2018). Furthermore, Geris et al. (2017) proved that for most species, there is no isotopic
68 fractionation during the process of RWU and transportation along the conduit before transpiration, making it
69 possible to specify plant water sources and water uptake patterns.

70 The water transport process through the soil-plant atmosphere continuum (SPAC) has been widely studied in
71 the context of water phase transition and movement and in many contexts. Compared to *Artemisia gmelinii*, *Vitex*
72 *negundo* obtained more water from deeper soils as the water stress increased, showed more flexibility to acclimate
73 the drought (Wang et al., 2017). Precipitation, soil water and stem water were sampled for analyses, Chang et al.



74 (2019) studied the water use strategies of four vegetation types after succession in the Loess Plateau and found that
75 the soil water used by different vegetation types both extended deeper with the development of succession, and
76 water was accessed from deeper and shallower soil during dry and wet seasons, respectively. Wang et al. (2021a)
77 investigated water use characteristics of *Robinia pseudoacacia* in plantations of 18 and 30 years, and found 30-yr
78 *R. pseudoacacia* mainly took water from shallow soil, while 18-yr *R. pseudoacacia* displayed variable responses to
79 variations in precipitation. These studies mainly focused on plants with yearly leaf abscission and studied the
80 seasonal variations generally, while studies concentrated in trees are relatively rare, especially comparisons between
81 different species, and there is a lack of understanding of the responses under different hydrological conditions. Thus,
82 investigation of the mainly artificially planted trees, such as *R. pseudoacacia* and *Pinus tabulaeformis*, in the Loess
83 Plateau would provide a scientific basis for forest management.

84 Three classes of approaches have been developed and used to determine the proportion of water sources
85 accessed by plants, which is the direct inference approach (Amin et al., 2020), the linear mixing models (Evaristo
86 et al., 2017) and Bayesian mixing models. Among them, the MixSIAR model (Bayesian mixing model) exhibited
87 good performance and prevailed in the assessment of plant water source apportionment (Beyer et al., 2018; Duvert
88 et al., 2021). The MixSIAR model has been directly applied to the Loess Plateau directly in many studies (Wang et
89 al., 2019; Tao et al., 2021; Wu et al., 2021), but has rarely been contrasted with other methods, e.g. the direct
90 inference approach and dynamics of soil moisture (Guo and Zhao, 2020). It is unclear whether the predicted results
91 obtained by one method is justified, which still need further comparisons with the variations in soil water.

92 In this study, we monitored the isotopic compositions of precipitation, soil, xylem, soil moisture and relevant
93 variables in *R. pseudoacacia* and *P. tabulaeformis* plantations from 2019–2020 in the Loess Plateau of China. The
94 objectives of this study were: (1) to investigate the spatial and temporal variations of stable isotopes in consecutive
95 hydrological years; (2) to quantify seasonal variations of RWU modes for the two main planted species; and (3) to
96 provide a scientific basis for the optimization of plantations with the combination of soil water storage (SWS).



97 2. Materials and methods

98 2.1 Study site

99 The experiment was carried out during 2019–2020 in the Caijiachuan catchment on the southeast of the Loess
100 Plateau, China (110°40′–110°48′E, 36°14′–36°18′N), which has an average altitude of 1168 m. The *R. pseudoacacia*
101 and *P. tabulaeformis* plantations were widely planted since implementation of the “Grain for Green” project. The
102 climate is temperate continental, with a mean annual precipitation of 491.6 mm in the period 1985–2020. More than
103 half of the annual precipitation is concentrated from July to September. The annual average potential
104 evapotranspiration is approximately 1723.9 mm. The groundwater table depth is far below 30 m in this area.

105 The soil is mainly classified as an Alfisol according to the USDA classification system. To weaken the impact
106 of other factors except tree species, we chose sample plots with good growth, similar tree-age and slope aspect, and
107 low human interference. The basic description of the experimental site was shown in Figure 1 and Table 1.

108 [Figure 1]

109 [Table 1]

110 2.2 Measurements and sampling

111 2.2.1 Meteorological measurements

112 An automatic weather station that monitored air temperature (T_a), precipitation (P, TR-525M-R1, Texas
113 Electronics, Inc. USA), relative humidity (RH), solar radiation (R_a) and wind speed (W_s) at 1 h intervals was located
114 below the hill (with the altitude of 1089 m), which was about 1.5 km away from the study sites. However, because
115 of instrument maintenance, meteorological data from September 9 to November 1 in 2020 was not collected.

116 2.2.2 Water sampling

117 Based on the tally method for sample plots of 10×10 m² of *R. pseudoacacia* (*R.*) and *P. tabulaeformis* (*P.*)
118 forest (Figure 1 (c)), two sample trees were chosen for sampling from each plantation species. During July–August
119 and October, which was regarded as the main growth reason and the end of growth reason, respectively, precipitation,



120 soil water and stem water were sampled for hydrogen and oxygen stable isotopes analysis.

121 Two homemade rainfall collectors were used to collect precipitation samples, which consisted of a 500 ml
122 polyethylene bottle and a 200 ml funnel; a ping-pang ball was loosely placed in the funnel to avoid evaporation.
123 Precipitation samples were gathered into two 10 ml polyethylene vials after rainfall events (> 2 mm). We selected
124 and cut suberized branches in the middle and upper canopy with mature bark (0.5–1.0 cm in diameter, 4–5 cm in
125 length) of *R. pseudoacacia* and *P. tabulaeformis*; xylem water was sampled 1–2 times per month at the same time
126 of day (13:00–15:00). Bark was quickly removed from the sampled twig, and stored twig in a 50 ml polyethylene
127 vial with three replicates. Meanwhile, after discarding the first 3 cm of soil to avoid sampling isotopically enriched
128 water because of evaporation, soil was sampled by auger around the sample tree with three replicates. The fresh soil
129 sample was divided into two parts, one was used to calculate soil water content (SWC) by the oven drying method
130 (105°C, 24 h), with 10 (0–20, 20–40, 40–60, 60–80, 80–100, 100–120, 120–140, 140–160, 160–180 and 180–200
131 cm) and 13 (0–5, 5–10, 10–15, 15–20, 20–40, 40–60, 60–80, 80–100, 100–120, 120–140, 140–160, 160–180 and
132 180–200 cm) soil layer depths in 2019 and 2020, respectively; the other part was stored in a 50 ml polyethylene
133 vial. All samples were numbered and sealed with parafilm® and stored in a refrigerator at –4°C before extraction.
134 In total, 54 precipitation samples, 54 xylem water samples, and 624 soil water samples were collected.

135 2.2.3 Isotopic analysis

136 An automated cryogenic vacuum distillation system (BJJL-2200, Beijing Jianling Technology limited, Beijing,
137 China) was used to extract soil and stem water in the lab, with cryogenic and heating temperatures of –20°C and
138 110°C, respectively; the extraction time and efficiency was 8 h and about 98.0%, respectively. After that, the
139 extracted water samples and precipitation samples were filtered by needle filter (Polyethersulfone (PES), 0.22 µm,
140 Membrana company, Germany), and stored in a refrigerator at 3°C before isotopic analysis. A cavity ring-down
141 spectroscopy (CRDS) isotopic water analyzer (L2140-i, Picarro Inc. USA) was used for water isotopic
142 measurements ($\delta^2\text{H}$ and $\delta^{18}\text{O}$). Results were expressed as parts per thousand relative to the Vienna Standard Mean



143 Ocean Water (V-SMOW), as in Eq. 1:

$$144 \quad \delta_{sample} = \left(\frac{R_{sample}}{R_{V-SMOW}} - 1 \right) \times 1000\text{‰} \quad (1)$$

145 where R_{sample} and R_{V-SMOW} are the isotope molar ratios of heavy to light isotopes ($^2\text{H}/^1\text{H}$, $^{18}\text{O}/^{16}\text{O}$) in water
146 samples and in V-SMOW, respectively. Precision of the CRDS analyzer was $\sim 0.1\text{‰}$ for $\delta^2\text{H}$ and $\sim 0.025\text{‰}$ for $\delta^{18}\text{O}$.

147 To specify the water source of the plant, after the SWC was standardized by z-score, hierarchical cluster
148 analysis (HCA) method was used to divide the soil layers into four parts based on Ward's method (Figure S1), which
149 was (1) 0–20 cm; (2) 20–40 cm; (3) 40–100 cm; and (4) 100–200 cm. The details can be seen in Zhao et al. (2018).

150 The isotope value of each soil layer was calculated by the soil water content weighted mean method
151 (Mahindawansa et al., 2018), as shown bellows:

$$152 \quad \delta_{i,j} = \frac{\sum_{i=1}^n \sum_{j=1}^3 \delta_{i,j} * SWC_j}{\sum_{i=1}^n \sum_{j=1}^3 SWC_j} \quad (2)$$

153 where $\delta_{i,j}$ is the representative isotopic compositions of the i_{th} soil layer; i is the number of soil layers in the i_{th}
154 soil layer, and $1 \leq n \leq 5$; j is the number of samples of the i_{th} soil layer in practice, and $\delta_{i,j}$ and SWC_j is the
155 corresponding raw isotopic value and soil water content of the sample, respectively.

156 2.2.4 The direct inference approach and parameter setting in MixSIAR

157 We assumed that the time delays between sampling and water transport were not significant. The direct
158 inference approach was applied by directly comparing $\delta^2\text{H}$ and $\delta^{18}\text{O}$ between soil and stem. The raw value of $\delta^{18}\text{O}$
159 for stem water and soil water in each interval were applied in this method.

160 After compared the raw and representative isotope values, the difference between the two values was generally
161 not significant (Figure S2). Considering the raw data applied in the direct inference approach, the raw isotope values
162 were also applied in the MixSIAR model for consistent. To determine the contribution of each source to the mixture,
163 the MixSIAR model, which was based on the Bayesian model principle, was applied to quantify the relative RWU
164 ratio of different soil water source (0–20, 20–40, 40–100 and 100–200 cm). The mean value and standard deviation
165 (SD) of isotopic composition of soil water (the source data) and raw plant xylem water (the mixture data) were input



166 into the model, and the fractionation coefficient was set to zero. The run length was set as “very long” for
167 convergence, and the model error was evaluated by residual error.

168 2.2.5 Plant water consumption

169 Based on the assumption of negligible surface runoff for the two forests, the water consumption of *R.*
170 *pseudoacacia* and *P. tabulaeformis* plantation was calculated by the water balance equation, as shown bellows:

$$171 \quad \Delta SWS = \sum \frac{10\Delta(SWC_i d_i)h}{\rho} \quad (3)$$

$$172 \quad ET = P - \Delta SWS \quad (4)$$

173 where ΔSWS is the dynamics of layer-cumulated SWS in the 0–200 cm soil layers (mm) during a certain time;
174 SWC_i represents the gravimetric soil moisture (%) in the soil layer; d_i indicates the soil bulk density (g/cm^3); h
175 represents the thickness of the soil layer; ρ is the density of water ($1 \text{ g}/\text{cm}^3$); i indicates the number of soil layers.
176 ET is the water consumption per plantations (mm).

177 2.3 Data analysis

178 The vapor pressure deficit (VPD) was calculated by the Tetens equation (Gimenez et al., 2019), and the FAO-
179 56 Penman-Monteith equation was used to estimate the reference evapotranspiration (ET_0). Groundwater was not
180 considered in our study, because groundwater table was well below 30 m in this area and not likely reached by *R.*
181 *pseudoacacia* and *P. tabulaeformis*.

182 The mean values of SWC, $\delta^{18}\text{O}$ and $\delta^2\text{H}$ both calculated by the weighted average method. A one-way ANOVA
183 paired by the least significant difference (LSD) test was performed to identify the differences of the SWC and
184 isotopic compositions of precipitation, soil and stem water between treatments (*R. pseudoacacia* and *P.*
185 *tabulaeformis*, drought and humid year). Pearson correlation was conducted to explore correlations between $\delta^{18}\text{O}$,
186 precipitation and temperature. All statistical analyses were conducted in R 4.0.3 and MATLAB R2018b.

187 3. Results

188 3.1 Temporal variation of environmental variables



189 Air temperature increased from mid-January to July and decreased from August to January of the next year;
190 the maximum daily mean temperature was 27.94°C in July 2019 and 26.34°C in August 2020 (Figure 2 (a)). There
191 was 420.0 mm precipitation in 2019 and 605.4 mm in 2020, mainly concentrated in the period July to September;
192 the precipitation within this period was 242.3 and 371.2 mm in 2019 and 2020, respectively. Meanwhile, the ET_0
193 was 903.17 mm in 2019 and more than 882.36 in 2020, and both highly during June to August (Figure 2 (b)). The
194 VPD was greater during May to July, which was 0.18–1.75 kPa and 0.20–1.75 kPa in 2019 and 2020, respectively.
195 Furthermore, according to the Standardized Precipitation Index (SPI, Figure S3) (McKee et al., 1993), 2019 and
196 2020 were classified as mild drought and mild humid years, respectively.

197 [Figure 2]

198 3.2 Dynamics of soil water and water consumption

199 Variations in soil water storage (ΔSWS) were calculated for *R. pseudoacacia* and *P. tabulaeformis* forest
200 (Figure 3). Under the same precipitation, the SWS of *R. pseudoacacia* and *P. tabulaeformis* forest from July to
201 October increased by 92.42 and 110.60 mm in 2019, and 46.01 and 100.26 mm in 2020, respectively. *R.*
202 *pseudoacacia* depleted soil water at 100–200 cm from July to August in both 2019 and 2020, while the SWS of 0–
203 100 cm increased both for *R. pseudoacacia* and *P. tabulaeformis* from August to October in 2019 because of the
204 increased precipitation during this period. *R. pseudoacacia* and *P. tabulaeformis* also depleted water from the 20–
205 100 cm and 0–20 cm soil layers, respectively, from August to October in 2020. Both plantations increased SWS
206 from shallow to deep soil layers over time in 2020. Moreover, the rate of increase in SWS generally decreased with
207 increasing soil depth in 2019, while the SWS of 40–100 and 100–200 cm soil depths increased more in 2020. For
208 example, the rates of increases of SWS were 1.10, 0.86, 0.64 and 0.06 for *R. pseudoacacia* forest at soil depths of
209 0–20, 20–40, 40–100 and 100–200 cm from July to October in 2019, and 0.01, 0.06, 0.14 and 0.21, respectively, in
210 2020.

211 [Figure 3]



212 3.3 Isotopic composition of water samples

213 With reference to the Global Meteoric Water Line (GMWL, $\delta^2\text{H} = 8\delta^{18}\text{O} + 10$), the relationships between $\delta^2\text{H}$
214 and $\delta^{18}\text{O}$ in precipitation and soil water samples were explored (Figure 4). During 2019, the slope and intercept of
215 the Local Meteoric Water Line (LMWL) were 8.62 and 14.56, respectively, which was higher than those in GMWL,
216 while these two parameters of LMWL in 2020 were smaller than those of GMWL. Most of the soil water samples
217 of both *R. pseudoacacia* and *P. tabulaeformis* plantations fell on the bottom of GMWL, and the slope and intercept
218 of the soil water line (SWL) were also smaller than those in LMWL. The $\delta^{18}\text{O}$ values of xylem water of both *R.*
219 *pseudoacacia* and *P. tabulaeformis* were within the ranges of soil samples.

220 [Figure 4]

221 From the perspective of isotopic compositions of water samples (Table S1), the $\delta^{18}\text{O}$ of precipitation in 2019
222 ranged from -8.60 to -6.31‰ , with the mean value of -7.20‰ and standard deviation of 0.78‰ , while the $\delta^2\text{H}$
223 ranged from -61.88 to -40.41‰ , with the mean value of -47.54‰ and standard deviation of 7.23‰ . The mean
224 $\delta^{18}\text{O}$ and $\delta^2\text{H}$ values of xylem water for *R. pseudoacacia* were -7.99 and -55.50‰ , respectively, and -6.76 and
225 -75.04‰ for *P. tabulaeformis*, respectively. The mean $\delta^{18}\text{O}$ value of precipitation, xylem of *R. pseudoacacia* and *P.*
226 *tabulaeformis* in 2020 was -10.05 , -5.29 and -4.82‰ , respectively, and -69.43 , -67.05 and -66.55‰ for $\delta^2\text{H}$,
227 respectively (Table S2). For total soil water samples of *R. pseudoacacia* in 2020, the mean values of $\delta^{18}\text{O}$ and $\delta^2\text{H}$
228 were $-10.32 \pm 1.81\text{‰}$ and $-72.99 \pm 12.12\text{‰}$, respectively, while they were $-8.70 \pm 1.33\text{‰}$ and $-66.16 \pm 8.16\text{‰}$ for *P.*
229 *tabulaeformis* soil water samples, respectively.

230 The maximum and minimum values of $\delta^{18}\text{O}$ and $\delta^2\text{H}$ both generally occurred in the 0–20 cm soil layers for
231 both tree species in 2019 (Table S1), and specifically occurred in the 5–10 cm soil layers in 2020 (Table S2).
232 Moreover, for both *R. pseudoacacia* and *P. tabulaeformis* plantations, the mean values of $\delta^{18}\text{O}$ and $\delta^2\text{H}$ of surface
233 soil layers were relatively high in 2019 and 2020, and water isotopic values were negatively correlated with soil
234 depth in general, although there was no clear difference in water isotopic values for the soil layers between 100–



235 200 cm.

236 3.4 Water uptake pattern based on the direct inference approach and MixSIAR model

237 Variations of $\delta^{18}\text{O}$ in the soil profile and stem during July, August and October in 2019 and 2020 are shown in
238 Figure 5. With increasing soil depth, the mean value of $\delta^{18}\text{O}$ generally first increased and then decreased, and the
239 soil moisture decreased gradually, except for the SWC in deep soil layers, which was relatively high for *P.*
240 *tabulaeformis* in July and August 2019.

241 [Figure 5]

242 During 2019, *R. pseudoacacia* mainly absorbed water from soil layers of 40–60 and 60–80 cm in July and
243 August (Figure 5 (a), (b)), respectively, while *P. tabulaeformis* always absorbed water from the 40–60 cm soil layer.
244 Both tree species absorbed water from 40–60 cm and deeper soil layers in October (Figure 5 (c)), although the SWC
245 in the 0–60 cm layer increased substantially from August to October. During 2020, water was mainly supplied to
246 both tree species from the soil layers deeper than 40 cm in July and August (Figure 5 (d), (e)), besides this, water
247 was absorbed from the surface soil layers by *R. pseudoacacia* in July and by *P. tabulaeformis* in August. Water
248 absorption was finally concentrated in the soil surface with the continuous increase in SWC (Figure 5 (f)). However,
249 the method had serious limitations in that it could only roughly determine the soil layers contributing to water
250 absorption and couldn't quantify the contribution of different soil layers.

251 Based on the results of MixSIAR model, the contributions of soil water sources from different soil layers to *R.*
252 *pseudoacacia* and *P. tabulaeformis* varied over time (Figure 6). During 2019, *R. pseudoacacia* evenly absorbed
253 water from soil layers of 0–20, 20–40, 40–100 and 100–200 cm in July, while *P. tabulaeformis* mainly absorbed
254 water from 0–20 and 20–40 cm with proportions of 0.37 and 0.36, respectively. The 100–200 cm soil layer
255 contributed more than half of the water absorbed by *R. pseudoacacia* in August, while *P. tabulaeformis* still mainly
256 absorbed water from the 0–40 cm soil layer. Lastly, the 40–100 and 100–200 cm soil layers contributed the most to
257 the both tree species in October. Similar to the results of the direct inference approach, *R. pseudoacacia* and *P.*



258 *tabulaeformis* both absorbed water from deep to shallow soil depth over time during 2020. The 100–200 cm soil
259 layer contributed 0.39 and 0.65 to *R. pseudoacacia* and *P. tabulaeformis* in July, respectively, and the 40–100 cm
260 soil layer contributed the most in August. While the 0–20 cm soil layer contributed substantially to both *R.*
261 *pseudoacacia* and *P. tabulaeformis* in October, with contribution rates of 0.36 and 0.31, respectively.

262 [Figure 6]

263 4. Discussion

264 4.1 Comparison of the water stable isotope composition of precipitation, soil and xylem

265 Precipitation was the main input to the regional water cycle, and the water stable isotope compositions reflected
266 the processes of water vapor transport. The slope and intercept of LMWL were higher than those of GMWL in 2019
267 (Figure 4), especially the intercept, indicating the larger unbalanced fractionation of water isotopes during the phase
268 change between vapor and precipitation in 2019. The slope and intercept were 7.65 and 7.48 in 2020, respectively.
269 This might have been caused by the effect of below-cloud evaporation (Wang et al., 2021b; Xiao et al., 2020). While
270 the precipitation in 2019 was mainly concentrated in September to October (97.7 mm from July to August, 215.0
271 mm from September to October), the precipitation samples were mainly sampled from July to August, which were
272 small and short duration rainfall events (Figure 2 (a)), most likely formed by regional moisture convection (Yamada
273 and Kurita, 2008; Lynn et al., 1998). The precipitation distribution reversed in 2020 (342.8 mm from July to August,
274 63.6 mm from September to October), which was highly affected by secondary evaporation, and the high
275 precipitation resulted in depleted isotope values (Lemma et al., 2020).

276 The relationship between temperature, precipitation and $\delta^{18}\text{O}$ was shown in Table 2.

277 [Table 2]

278 Increased temperature and precipitation caused higher and lower isotope values, respectively (Wan et al., 2018;
279 Dody and Ziv, 2013). This tendency was also demonstrated by the mean value of $\delta^{18}\text{O}$, which was lower and
280 significantly higher than -10.0‰ in 2020 and 2019, respectively (Tables S1 and S2).



281 From the perspective of the SWL (Figure 4), the soil water isotopic values distributed around LMWL, and the
282 slope and intercept of both *R. pseudoacacia* and *P. tabulaeformis* plantation were lower than those in LMWL,
283 indicating that the soil water mainly originated from atmospheric rainfall and intense soil evaporation that occurred
284 during our study (Liu et al., 2021). Specifically, $\delta^{18}\text{O}$ was enriched in the 0–20 cm soil layer in July in both 2019
285 and 2020 (Figure 5 (a) and (d)), which was caused by the arid climate and rare precipitation prior to this study. This
286 tendency continued through to August in 2019, while the $\delta^{18}\text{O}$ values in the 0–40 cm soil layer became smaller from
287 July to August in 2020 because the precipitation in 2020 within this period was 2.47 times more than that in 2019.
288 The new precipitation replenished the soil surface, and pushed the “old” water deeper into the soil profile (Xiang et
289 al., 2019). This phenomenon was amplified from August to October (Figure 5 (c), (f)). Yang and Fu (2017) proved
290 that soil water migration in the Loess Plateau was dominated by piston flow, while rare rainwater infiltrated deeper
291 into the soil profile in the form of preferential flow, and new water (precipitation) evenly mixed with old water (soil
292 water). The $\delta^{18}\text{O}$ values below 100 cm were relatively stable (Figure 5), indicating that they were barely influenced
293 by precipitation. Furthermore, the vertical distribution of $\delta^{18}\text{O}$ in *R. pseudoacacia* plantation was less than that of
294 *P. tabulaeformis* in 2020, indicating that evaporation under *P. tabulaeformis* was more intense than that under *R.*
295 *pseudoacacia* during a mild humid year, partially because of the small leaf area of conifer species and relatively
296 loose stand density (Table 1).

297 4.2 Comparison of the results of the direct inference approach and MixSIAR model

298 The direct inference approach suggested that both *R. pseudoacacia* and *P. tabulaeformis* absorbed water from
299 the 40–100 cm soil layer in July and August, and *P. tabulaeformis* also consumed soil water below 100 cm in October
300 2019 (Figure 5). While both shallow and deep soil supplied water to plants in July and August, and they mainly
301 absorbed soil water from 0–20 cm soil depth in October 2020. However, the MixSIAR model pointed that in 2019
302 (mild drought year), *R. pseudoacacia* absorbed water evenly from different soil layers (0–20, 20–40, 40–100, 100–
303 200 cm) in July, and absorbed more than half of the total water from the 100–200 cm soil layer in August, while the



304 depth of absorption shrank to 40–100 cm in October (Figure 6). Using the MixSIAR model, Zhao et al. (2020) also
305 found that *R. pseudoacacia* preferred deep soil water to support tree growth and nutrient absorption during the dry
306 season. Our study demonstrated that *P. tabulaeformis* mainly absorbed water at the soil surface (0–40 cm) in July
307 and August, then extended to soil layers deeper than 100 cm in October; this result was consistent with that of Duan
308 et al. (2008), who found that *P. tabulaeformis* derived much of its water from rainwater (surface soil) during the
309 growth season. The two trees had different RWU modes during the drought year, mainly caused by different root
310 distribution and water availability. Zhou and Shangguan (2006) found that the roots of *P. tabulaeformis* mainly
311 distributed in the 0–15 cm soil layer and their density decreased with increasing soil depth. However, the root length
312 and biomass of *R. pseudoacacia* was significantly greater than that of *P. tabulaeformis*, and *R. pseudoacacia* showed
313 strong drought resistance for its broad and deep root systems (Zhang et al., 2014). *R. pseudoacacia* had a larger
314 range of soil for water absorption than *P. tabulaeformis*. Moreover, the root vigor gradually decreased with a
315 decrease in SWC (Li et al., 2011), so the activity of the shallow root system was weakened because of low
316 precipitation. Thus, *R. pseudoacacia* was able to use deep soil water during the drought year. The trend of water
317 absorption for both tree species was from deep soil layers (100–200 cm) to shallow soil layers (40–100 cm) to
318 surface soil (0–20 cm) from July to August to October in 2020 (mild humid year, Figure 6), which was similar to
319 the results of the direct inference approach. In contrast, the results of the two methods were not completely consistent,
320 especially during the drought year, which could potentially be explained by the different performance of different
321 species under diverse environmental stressors.

322 From the perspective of Δ SWS, the SWS of the 20–100 cm soil layer decreased for the two plantations from
323 July to August in 2019 (Figure 3), and *R. pseudoacacia* also consumed substantial water from soil layers below 100
324 cm. This was clearly indicated by the results of the MixSIAR model (Figure 6), where the contribution rates of the
325 100–200 cm soil layers were 0.24 and 0.52 in July and August, respectively. Moreover, the results of MixSIAR were
326 more specific and coordinated with the dynamics of SWS in 2020, for example, the contribution rate of the 20–100



327 cm soil layer to *R. pseudoacacia* was considerable in October, while the direct inference approach manifested the
328 surface soil only, although it indicated the upward trend of the main soil layer supplying water to *R. pseudoacacia*
329 from July to October (Figure 5). Tetzlaff et al. (2021) also found that the isotopic values of xylem water were usually
330 dissimilar to those of soil water in the drier months, which weakened the applicability of the direct inference
331 approach. In general, the MixSIAR model was more accurate and applicable in the study of water uptake mode for
332 this region.

333 To explore the relationship between SWC and RWU, a correlation analysis was conducted between SWC and
334 contribution rates (based on the MixSIAR model) of the 0–20, 20–40, 40–100 and 100–200 cm soil layers. The
335 results showed that the correlation between the two was not significant, indicating that the process of RWU was a
336 combination of many factors, including SWC, root distribution, soil properties and meteorological factors (Zhao et
337 al., 2020). While there was a tendency that the increasement of SWC facilitated the contribution rates for *R.*
338 *pseudoacacia*, as shown below:

$$339 \quad \Delta CR = 1.07 \times \Delta SWC - 0.33 \quad R^2 = 0.73 \quad (4)$$

340 where ΔCR and ΔSWC were the degree of change in the contribution rates (CR) and SWC, respectively. While
341 this trend was not clear for *P. tabulaeformis*.

342 4.3 Plant water consumption and management

343 The SWS of the 0–40 cm soil layer from August to October in 2019, the 20–40 cm soil layer from July to
344 August and the 40–200 cm soil layer from August to October in 2020 showed the greatest increase (Figure 3),
345 meaning that water was only restored in shallower soil during the mild drought year, while it continuously infiltrated
346 to deeper soil during the mild humid year. In total, the SWS of *P. tabulaeformis* plantation increased more than that
347 of *R. pseudoacacia* from July to October, especially during the mild humid year (in 2020), indicating that *R.*
348 *pseudoacacia* consumed more water than *P. tabulaeformis* after neglecting the differences in surface runoff and soil
349 evaporation (Jian et al., 2015; Shen et al., 2020). Both species consumed more water in the humid year than in the



350 drought year, demonstrated by the similar SWS at the end of the growth season under increased precipitation from
351 2019 to 2020.

352 When combined with the results of water apportionment, *R. pseudoacacia* water absorption extended to deeper
353 soil layers when the water supply was insufficient, while *P. tabulaeformis* water absorption was restricted to the
354 surface soil (0–40 cm). With the supply of large precipitation volumes, the main soil layers of RWU for *R.*
355 *pseudoacacia* shrank to surface. However, both species absorbed water from deep to shallow soil layers with
356 continuous sufficient water supply by rainfall through to the end of growth season. In summary, the water use
357 strategy of *P. tabulaeformis* was conservative, while it was more alterable and hydrotactic for *R. pseudoacacia*.

358 Our study found that the reference evapotranspiration was greater than annual precipitation in this region.
359 However, countless trees with high density were planted during the afforestation programs, without considering the
360 limited precipitation (Jia et al., 2017). Increasing canopy transpiration and interception both highly weakened the
361 soil water storage, the plants with deeper root systems were promoted to absorb water from deep soil layers to
362 alleviate water stress. With the characteristics of well-developed roots, *R. pseudoacacia* had a higher resilience
363 under drought. Furthermore, *R. pseudoacacia* consumed more water throughout the growing season, especially from
364 deep soil layers (100–200 cm), causing potential threat for soil desiccation, and led to imbalanced water cycle and
365 ecological degradation. Compare to the *R. pseudoacacia*, *P. tabulaeformis* consumed less water than *R.*
366 *pseudoacacia*. However, *P. tabulaeformis* preferred to absorb water from shallow soil layers, which growth may be
367 limited by precipitation. The continuous absorption from shallow soil would plunder the water sources from
368 understory vegetations, and may not conducive to the construction of functional ecological forest.

369 Considering the regional water conservation and water cycle, the artificial *P. tabulaeformis* plantation was
370 better than the *R. pseudoacacia*. However, a combination of different plant species with different water use strategies
371 would form a good community, which would also good for the long-term and sustainable development of forest
372 ecosystems. And reasonable thinning should be applied for artificial plantations, which needs further detailed



373 research.

374 5. Conclusions

375 In this study, we explored the spatial and temporal variations of water stable isotopes of precipitation, soil
376 water and xylem, and we investigated the water uptake patterns of *R. pseudoacacia* and *P. tabulaeformis* by means
377 of the direct inference approach and the MixSIAR model, and taking the variations in SWS as a reference. The $\delta^{18}\text{O}$
378 values of precipitation were positively and significantly negatively correlated with temperature and precipitation
379 volume, respectively. The isotopic compositions of surface soil water varied with seasons, while those of the soil
380 layers below 100 cm were relatively stable.

381 Compared with the direct inference approach, the MixSIAR model performed better in quantifying dynamics
382 of RWU modes; and was consistent with the variations in SWS. The model results showed that *R. pseudoacacia*
383 and *P. tabulaeformis* had different RWU modes, especially in a drought year. *R. pseudoacacia* mainly absorbed
384 water from the 100–200 cm soil layer in the drought season, and *R. pseudoacacia* showed strong drought resilience
385 with the flexible water use strategies, while *P. tabulaeformis* consumed water mainly from the 0–40 cm soil layer
386 under drought. However, the water absorption for both tree species changed from deep soil (100–200 cm) to shallow
387 soil (0–40 cm) with continuous water input during the humid year. Furthermore, *R. pseudoacacia* consumed more
388 water than *P. tabulaeformis*, especially in the mild humid year, and preferred to extract deep soil water in the drought
389 year, which could induce soil desiccation and be harmful to the sustainable development of forest ecosystems. This
390 study evaluated water use characteristics of two mainly planted trees in Chinese Loess Plateau, and provides
391 scientific basis for plant species selection and forest restoration and management.

392 **Code and Data availability.** Codes applied in the MixSIAR model are available upon request to the authors. Isotopic
393 data and data of soil water are available upon request to the authors.

394 **Author contributions.** Chengzhong Pan, Yongsheng Cui and Lan Ma designed the research. Yongsheng Cui and
395 Zhanwei Sun conducted the experiment and collected the data. Zhanwei Sun made some data curation, Yongsheng



396 Cui analyzed the data and wrote the original manuscript. Chengzhong Pan and Lan Ma provided suggestions to the
397 original manuscript.

398 **Conflict of interest.** The authors declare that they have no conflict of interest.

399 **Acknowledgements.** This research was financially supported by the National Natural Science Foundation of China
400 (Grants 42077059 and 41771305).

401 References

- 402 Amin, A., Zuecco, G., Geris, J., Schwendenmann, L., McDonnell, J. J., Borga, M., and Penna, D.: Depth distribution of
403 soil water sourced by plants at the global scale: A new direct inference approach, *Ecohydrology*, 13, 10.1002/eco.2177,
404 2020.
- 405 Barnes, C. J. and Allison, G. B.: Tracing of water movement in the unsaturated zone using stable isotopes of hydrogen
406 and oxygen, *Journal of Hydrology*, 100, 143-176, 10.1016/0022-1694(88)90184-9, 1988.
- 407 Beyer, M., Hamutoko, J. T., Wanke, H., Gaj, M., and Koening, P.: Examination of deep root water uptake using anomalies
408 of soil water stable isotopes, depth-controlled isotopic labeling and mixing models, *Journal of Hydrology*, 566, 122-136,
409 10.1016/j.jhydrol.2018.08.060, 2018.
- 410 Chang, E., Li, P., Li, Z., Xiao, L., Zhao, B., Su, Y., and Feng, Z.: Using water isotopes to analyze water uptake during
411 vegetation succession on abandoned cropland on the Loess Plateau, China, *Catena*, 181, 10.1016/j.catena.2019.104095,
412 2019.
- 413 Dai, J., Zhang, X., Luo, Z., Wang, R., Liu, Z., He, X., Rao, Z., and Guan, H.: Variation of the stable isotopes of water in
414 the soil-plant-atmosphere continuum of a *Cinnamomum camphora* woodland in the East Asian monsoon region, *Journal*
415 *of Hydrology*, 589, 10.1016/j.jhydrol.2020.125199, 2020.
- 416 Dody, A. and Ziv, B.: Factors affecting isotopic composition of the rainwater in the Negev Desert, Israel, *Journal of*
417 *Geophysical Research: Atmospheres*, 118, 8274-8284, 10.1002/jgrd.50592, 2013.
- 418 Duan, D. Y., Ouyang, H., Song, M. H., and Hu, Q. W.: Water sources of dominant species in three alpine ecosystems on
419 the Tibetan Plateau, China, *J Integr Plant Biol*, 50, 257-264, 10.1111/j.1744-7909.2007.00633.x, 2008.
- 420 Duvert, C., Canham, C. A., Barbeta, A., Alvarez Cortes, D., Chandler, L., Harford, A. J., Leggett, A., Setterfield, S. A.,
421 Humphrey, C. L., and Hutley, L. B.: Deuterium depletion in xylem water and soil isotopic effects complicate the
422 assessment of riparian tree water sources in the seasonal tropics, *Ecohydrology*, 10.1002/eco.2383, 2021.
- 423 Evaristo, J., McDonnell, J. J., and Clemens, J.: Plant source water apportionment using stable isotopes: A comparison of
424 simple linear, two-compartment mixing model approaches, *Hydrological Processes*, 31, 3750-3758, 10.1002/hyp.11233,
425 2017.
- 426 Fang, X., Zhao, W., Wang, L., Feng, Q., Ding, J., Liu, Y., and Zhang, X.: Variations of deep soil moisture under different
427 vegetation types and influencing factors in a watershed of the Loess Plateau, China, *Hydrology and Earth System Sciences*,
428 20, 3309-3323, 10.5194/hess-20-3309-2016, 2016.
- 429 Geris, J., Tetzlaff, D., McDonnell, J. J., and Soulsby, C.: Spatial and temporal patterns of soil water storage and vegetation
430 water use in humid northern catchments, *Sci Total Environ*, 595, 486-493, 10.1016/j.scitotenv.2017.03.275, 2017.
- 431 Gimenez, B. O., Jardine, K. J., Higuchi, N., Negron-Juarez, R. I., Sampaio-Filho, I. J., Cobello, L. O., Fontes, C. G.,
432 Dawson, T. E., Varadharajan, C., Christianson, D. S., Spanner, G. C., Araujo, A. C., Warren, J. M., Newman, B. D., Holm,
433 J. A., Koven, C. D., McDowell, N. G., and Chambers, J. Q.: Species-Specific Shifts in Diurnal Sap Velocity Dynamics
434 and Hysteretic Behavior of Ecophysiological Variables During the 2015-2016 El Nino Event in the Amazon Forest, *Front*



- 435 Plant Sci, 10, 830, 10.3389/fpls.2019.00830, 2019.
- 436 Guo, H. and Zhao, Y.: Using isotopic labeling to investigate root water uptake in an alley cropping system within
437 Taklimakan Desert Oasis, China, *Agroforestry Systems*, 95, 907-918, 10.1007/s10457-020-00527-0, 2020.
- 438 Jackisch, C., Knoblauch, S., Blume, T., Zehe, E., and Hassler, S. K.: Estimates of tree root water uptake from soil moisture
439 profile dynamics, *Biogeosciences*, 17, 5787-5808, 10.5194/bg-17-5787-2020, 2020.
- 440 Jia, X., Shao, M. a., Zhu, Y., and Luo, Y.: Soil moisture decline due to afforestation across the Loess Plateau, China,
441 *Journal of Hydrology*, 546, 113-122, 10.1016/j.jhydrol.2017.01.011, 2017.
- 442 Jian, S., Zhao, C., Fang, S., and Yu, K.: Effects of different vegetation restoration on soil water storage and water balance
443 in the Chinese Loess Plateau, *Agricultural and Forest Meteorology*, 206, 85-96, 10.1016/j.agrformet.2015.03.009, 2015.
- 444 Lemma, B., Kebede Gurmessa, S., Nemomissa, S., Otte, I., Glaser, B., and Zech, M.: Spatial and temporal (2)H and (18)O
445 isotope variation of contemporary precipitation in the Bale Mountains, Ethiopia(), *Isotopes Environ Health Stud*, 56, 122-
446 135, 10.1080/10256016.2020.1717487, 2020.
- 447 Li, P., Zhao, h., Li, Z., and Xue, S.: Root distributions and drought resistance of plantation tree species on the Weibei
448 Loess Plateau in China, *African Journal of Agricultural Research*, 6, 4989-4997, 10.5897/AJAR11.832, 2011.
- 449 Liu, J., Wu, H., Cheng, Y., Jin, Z., and Hu, J.: Stable isotope analysis of soil and plant water in a pair of natural grassland
450 and understory of planted forestland on the Chinese Loess Plateau, *Agricultural Water Management*, 249,
451 10.1016/j.agwat.2021.106800, 2021.
- 452 Liu, Y., Miao, H.-T., Huang, Z., Cui, Z., He, H., Zheng, J., Han, F., Chang, X., and Wu, G.-L.: Soil water depletion patterns
453 of artificial forest species and ages on the Loess Plateau (China), *Forest Ecology and Management*, 417, 137-143,
454 10.1016/j.foreco.2018.03.005, 2018.
- 455 Lynn, B. H., Tao, W.-K., and Wetzell, P. J.: A Study of Landscape-Generated Deep Moist Convection, *Monthly Weather*
456 *Review*, 126, 928-942, 10.1175/1520-0493(1998)126<0928:ASOLGD>2.0.CO;2, 1998.
- 457 Ma, L., Teng, Y., and Shangguan, Z.: Ecohydrological responses to secondary natural *Populus davidiana* and plantation
458 *Pinus tabulaeformis* woodlands on the Loess Plateau of China, *Ecohydrology*, 7, 612-621, 10.1002/eco.1382, 2014.
- 459 Mahindawansa, A., Orłowski, N., Kraft, P., Rothfuss, Y., Racela, H., and Breuer, L.: Quantification of plant water uptake
460 by water stable isotopes in rice paddy systems, *Plant and Soil*, 429, 281-302, 10.1007/s11104-018-3693-7, 2018.
- 461 McKee, T. B., Doesken, N. J., and Kleist, J.: The relationship of drought frequency and duration to time scales, Eighth
462 Conference on Applied Climatology, Anaheim, California, 17-22 January 1993/1993.
- 463 Meißner, M., Köhler, M., Schwendenmann, L., Hölscher, D., and Dyckmans, J.: Soil water uptake by trees using water
464 stable isotopes ($\delta^2\text{H}$ and $\delta^{18}\text{O}$)—a method test regarding soil moisture, texture and carbonate, *Plant and Soil*, 376, 327-
465 335, 10.1007/s11104-013-1970-z, 2013.
- 466 Qiu, D., Gao, P., Mu, X., and Zhao, B.: Vertical variations and transport mechanism of soil moisture in response to
467 vegetation restoration on the Loess Plateau of China, *Hydrological Processes*, 35, e14397, 10.1002/hyp.14397, 2021.
- 468 Shen, M.-s., Zhang, J.-j., Zhang, S.-h., Zhang, H.-b., Sun, R.-x., and Zhang, Y.-z.: Seasonal variations in the influence of
469 vegetation cover on soil water on the loess hillslope, *Journal of Mountain Science*, 17, 2148-2160, 10.1007/s11629-019-
470 5942-5, 2020.
- 471 Tao, Z., Neil, E., and Si, B.: Determining deep root water uptake patterns with tree age in the Chinese loess area,
472 *Agricultural Water Management*, 249, 10.1016/j.agwat.2021.106810, 2021.
- 473 Tetzlaff, D., Buttle, J., Carey, S. K., Kohn, M. J., Laudon, H., McNamara, J. P., Smith, A., Sprenger, M., and Soulsby, C.:
474 Stable isotopes of water reveal differences in plant – soil water relationships across northern environments, *Hydrological*
475 *Processes*, 35, 10.1002/hyp.14023, 2021.
- 476 Wan, H., Liu, W., and Xing, M.: Isotopic composition of atmospheric precipitation and its tracing significance in the
477 Laohequ Basin, Loess plateau, China, *Sci Total Environ*, 640-641, 989-996, 10.1016/j.scitotenv.2018.05.338, 2018.
- 478 Wang, J., Fu, B., Lu, N., and Zhang, L.: Seasonal variation in water uptake patterns of three plant species based on stable
479 isotopes in the semi-arid Loess Plateau, *Sci Total Environ*, 609, 27-37, 10.1016/j.scitotenv.2017.07.133, 2017.



- 480 Wang, J., Fu, B., Lu, N., Wang, S., and Zhang, L.: Water use characteristics of native and exotic shrub species in the semi-
481 arid Loess Plateau using an isotope technique, *Agriculture, Ecosystems & Environment*, 276, 55-63,
482 10.1016/j.agee.2019.02.015, 2019.
- 483 Wang, J., Fu, B., Jiao, L., Lu, N., Li, J., Chen, W., and Wang, L.: Age-related water use characteristics of *Robinia*
484 *pseudoacacia* on the Loess Plateau, *Agricultural and Forest Meteorology*, 301-302, 10.1016/j.agrformet.2021.108344,
485 2021a.
- 486 Wang, S., Jiao, R., Zhang, M., Crawford, J., Hughes, C. E., and Chen, F.: Changes in Below-Cloud Evaporation Affect
487 Precipitation Isotopes During Five Decades of Warming Across China, *Journal of Geophysical Research: Atmospheres*,
488 126, 10.1029/2020JD033075, 2021b.
- 489 Wang, Y., Hu, W., Zhu, Y., Shao, M. a., Xiao, S., and Zhang, C.: Vertical distribution and temporal stability of soil water
490 in 21-m profiles under different land uses on the Loess Plateau in China, *Journal of Hydrology*, 527, 543-554,
491 10.1016/j.jhydrol.2015.05.010, 2015.
- 492 West, J. B., Bowen, G. J., Cerling, T. E., and Ehleringer, J. R.: Stable isotopes as one of nature's ecological recorders,
493 *Trends Ecol Evol*, 21, 408-414, 10.1016/j.tree.2006.04.002, 2006.
- 494 Wu, W., Li, H., Feng, H., Si, B., Chen, G., Meng, T., Li, Y., and Siddique, K. H. M.: Precipitation dominates the
495 transpiration of both the economic forest (*Malus pumila*) and ecological forest (*Robinia pseudoacacia*) on the Loess
496 Plateau after about 15 years of water depletion in deep soil, *Agricultural and Forest Meteorology*, 297,
497 10.1016/j.agrformet.2020.108244, 2021.
- 498 Xiang, W., Si, B. C., Biswas, A., and Li, Z.: Quantifying dual recharge mechanisms in deep unsaturated zone of Chinese
499 Loess Plateau using stable isotopes, *Geoderma*, 337, 773-781, 10.1016/j.geoderma.2018.10.006, 2019.
- 500 Xiao, H., Zhang, M., Wang, S., Che, C., Du, Q., Zhang, Y., Han, T., and Su, P.: Sub-cloud secondary evaporation effect
501 of precipitation isotope in Shaanxi-Gansu-Ningxia region, China (abstract in English), *Chinese Journal of Applied*
502 *Ecology*, 31, 3814-3822, 10.13287/j.1001-9332.202011.013, 2020.
- 503 Yamada, H. and Kurita, N.: The Role of Local Moisture Recycling Evaluated Using Stable Isotope Data from over the
504 Middle of the Tibetan Plateau during the Monsoon Season, *Journal of Hydrometeorology*, 9, 760-775,
505 10.1175/2007jhm945.1, 2008.
- 506 Yang, Y. and Fu, B.: Soil water migration in the unsaturated zone of semiarid region in China from isotope evidence,
507 *Hydrology and Earth System Sciences*, 21, 1757-1767, 10.5194/hess-21-1757-2017, 2017.
- 508 Zhang, C., Chen, L., and Jiang, J.: Vertical root distribution and root cohesion of typical tree species on the Loess Plateau,
509 China, *Journal of Arid Land*, 6, 601-611, 10.1007/s40333-014-0004-x, 2014.
- 510 Zhao, X., Li, F., Ai, Z., Li, J., and Gu, C.: Stable isotope evidences for identifying crop water uptake in a typical winter
511 wheat-summer maize rotation field in the North China Plain, *Sci Total Environ*, 618, 121-131,
512 10.1016/j.scitotenv.2017.10.315, 2018.
- 513 Zhao, Y., Wang, Y., He, M., Tong, Y., Zhou, J., Guo, X., Liu, J., and Zhang, X.: Transference of *Robinia pseudoacacia*
514 water-use patterns from deep to shallow soil layers during the transition period between the dry and rainy seasons in a
515 water-limited region, *Forest Ecology and Management*, 457, 10.1016/j.foreco.2019.117727, 2020.
- 516 Zhou, Z. and Shanguan, Z.: Vertical distribution of fine roots in relation to soil factors in *Pinus tabulaeformis* Carr. forest
517 of the Loess Plateau of China, *Plant and Soil*, 291, 119-129, 10.1007/s11104-006-9179-z, 2006.
- 518

519



520 Tables

521 Table 1 Basic description of the study sites

Site	Main plant type	Slope gradient (°)	Slope aspects (°)	Tree-age (yr)	Tree-height (m)	DBH (cm)	Stand density	Soil (0–200 cm)	
								Bulk density (g/cm ³)	Field capacity (g/g)
R. forestland	<i>Robinia pseudoacacia</i> ,	22	283	26	8.73±0.77	10.20±0.47	2×3.5 m	1.27	0.42
	<i>Rosa xanthina</i> ,								
	<i>Artemisia sacrorum</i> ,								
	<i>Carex spp.</i>								
P. forestland	<i>Pinus tabulaeformis</i> ,	23	315	29	6.73±0.42	11.06±0.43	2.5×4 m	1.25	0.42
	<i>Carex spp.</i>								

NOTE: DBH means the diameter of trees at 1.3 m above the ground. Values of the mean ± SD were presented.

522

523

524 Table 2 Relationships between temperature (T_a), precipitation volume (P) and $\delta^{18}\text{O}$

Year	2019		2020	
T_a - $\delta^{18}\text{O}$	$\delta^{18}\text{O} = 0.28T_a - 12.97$	$R^2 = 0.25$	$\delta^{18}\text{O} = 0.21T_a - 12.88$	$R^2 = 0.43 *$
P - $\delta^{18}\text{O}$	$\delta^{18}\text{O} = -0.11P - 6.03$	$R^2 = 0.76 *$	$\delta^{18}\text{O} = -0.22P - 7.65$	$R^2 = 0.54 **$

NOTE: * and ** means $P < 0.05$ and $P < 0.01$, respectively.

525

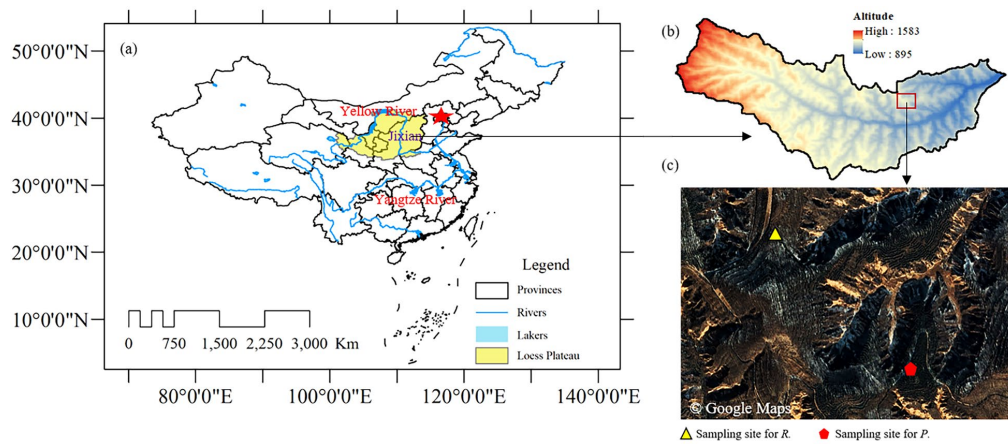
526



527 Figures

528

529



530

531 Figure 1 The study sites in Chinese Loess Plateau (a), and the Caijiachuan catchment (b). (c) google map of the
532 experimental sites for *Robinia pseudoacacia* (*R.*) and *Pinus tabulaeformis* (*P.*) plantations.

533

534

535

536

537

538

539

540

541

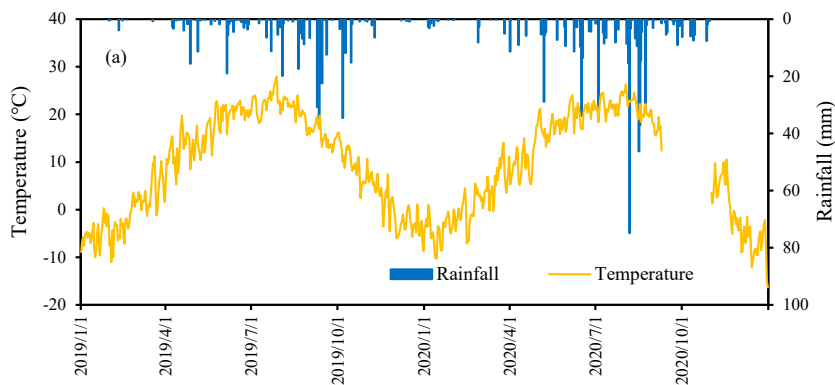
542

543

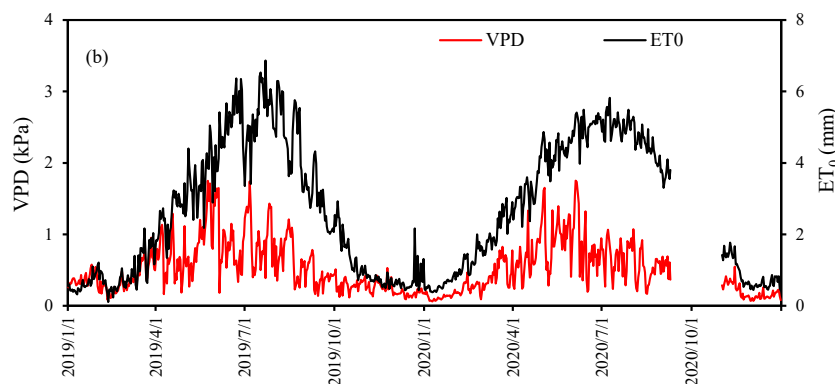


544

545



546



547

548 Figure 2 Daily dynamics of temperature, rainfall, vapor pressure deficit (VPD) and reference evapotranspiration
549 (ET_0) in 2019 and 2020.

550

551

552

553

554

555

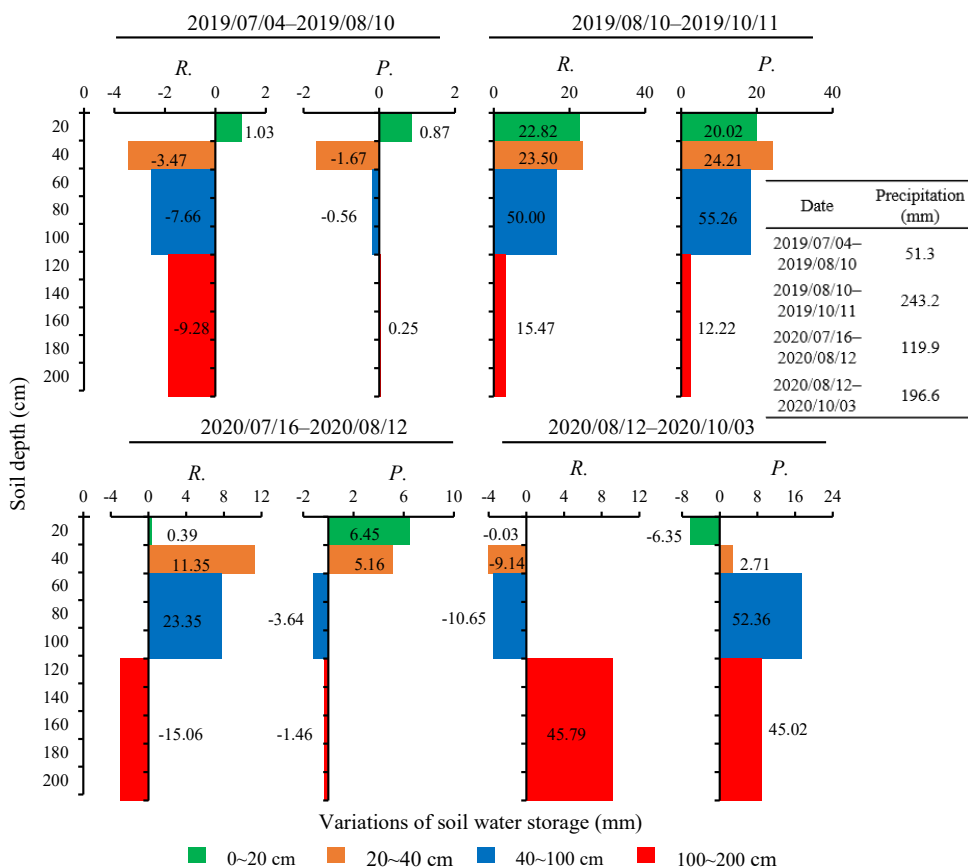
556

557



558

559



560

561 Figure 3 Variations of soil water storage (the area of the blocks) along the soil depths during our study (from July
 562 to October) for *R. pseudoacacia* (*R.*) and *P. tabulaeformis* (*P.*) plantation, and the number noted in the figure was
 563 the variations of soil water storage of different soil layers (0–20, 20–40, 40–100, 100–200 cm) at the corresponding
 564 time. The precipitation at the corresponding time was shown in the table.

565

566

567

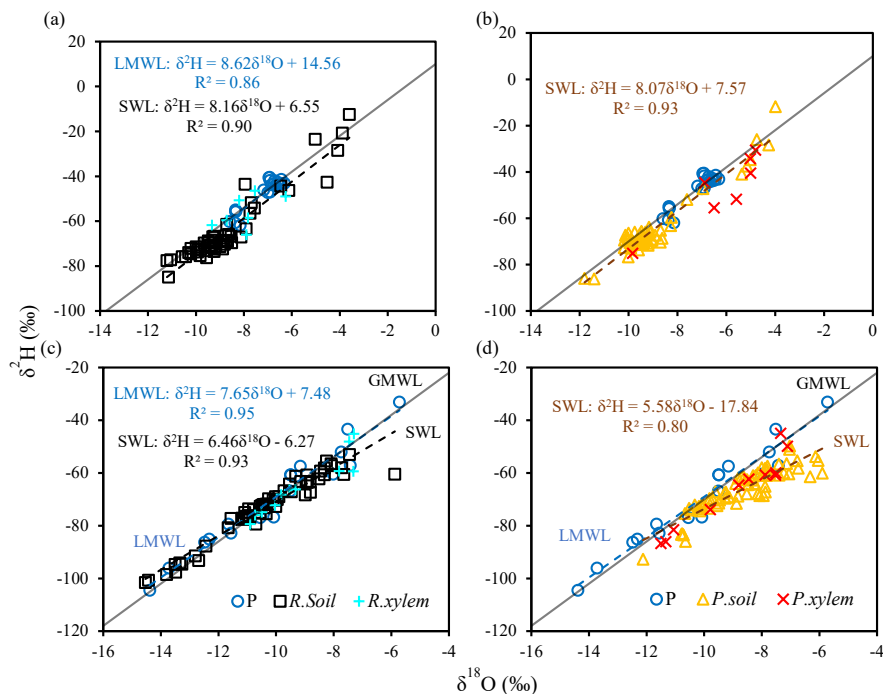
568

569



570

571



572

573 Figure 4 Relationship between $\delta^2\text{H}$ and $\delta^{18}\text{O}$ in precipitation (LMWL), soil water (SWL) and xylem water. (a)
 574 and (b) was *R. pseudoacacia* and *P. tabulaeformis* forest in 2019, respectively; (c) and (d) was *R. pseudoacacia* and
 575 *P. tabulaeformis* forest in 2020, respectively. And the grey solid line represents the Global Meteoric Water Line
 576 (GMWL), the blue, black and orange dashed line represents the LMWL, SWL of *R. pseudoacacia* and *P.*
 577 *tabulaeformis*, respectively.

578

579

580

581

582

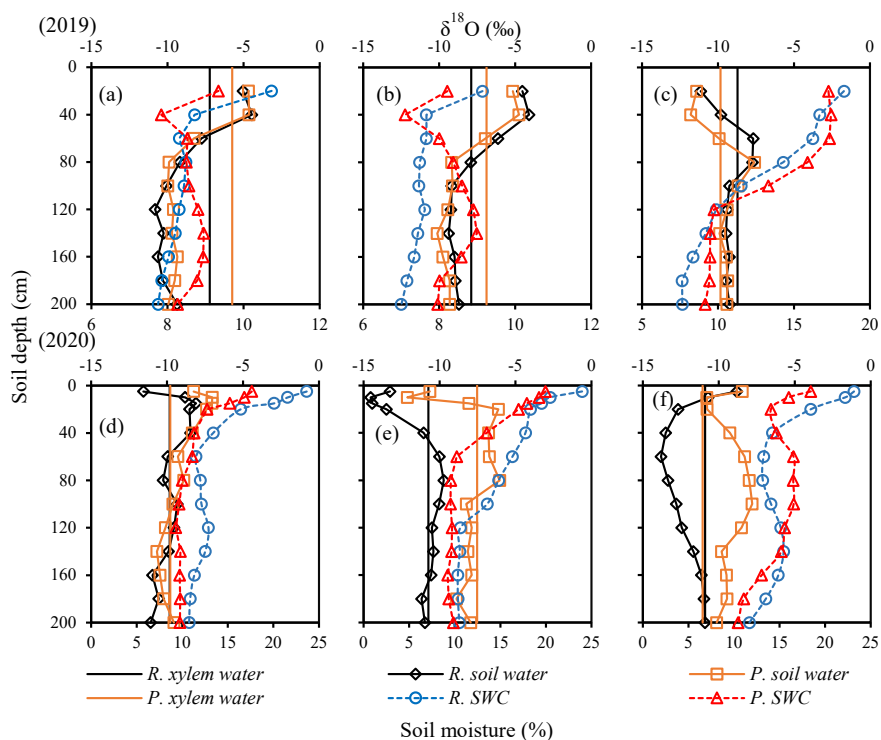
583

584



585

586



587

588 Figure 5 Mean values of $\delta^{18}\text{O}$ in xylem and soil water along the soil profile, and corresponding soil moisture for
589 *R. pseudoacacia* and *P. tabulaeformis* forest. (a) and (d), (b) and (e), (c) and (f) was the samples in July, August,
590 October in 2019 and 2020, respectively.

591

592

593

594

595

596

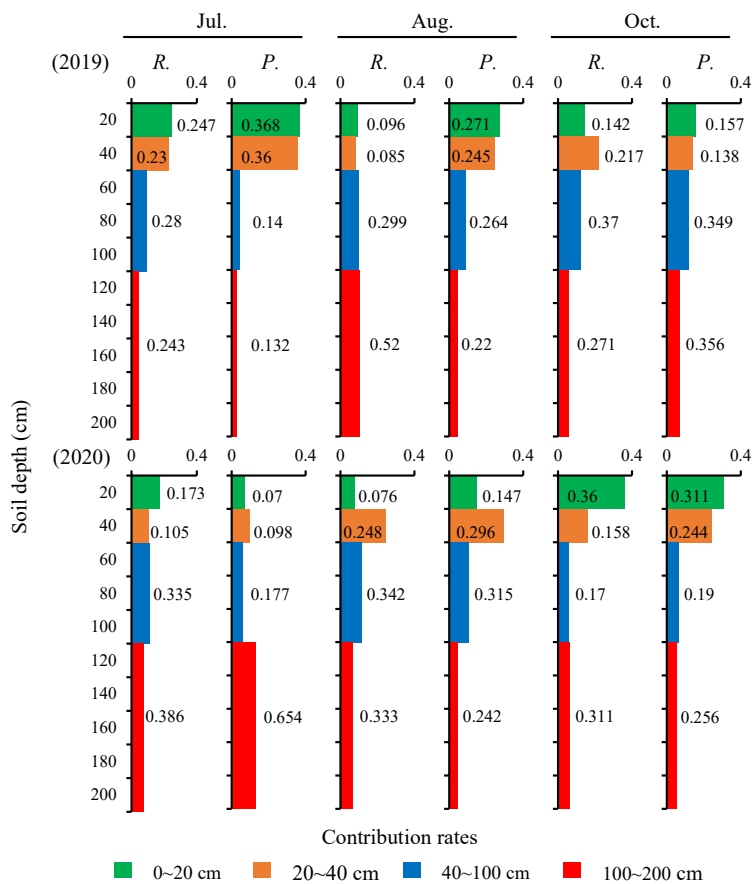
597

598



599

600



601

602 Figure 6 Contribution rates of soil water (the area of the blocks) to *R. pseudoacacia* (*R.*) and *P. tabulaeformis* (*P.*)

603 based on the MixSIAR model, according to the values of $\delta^{18}\text{O}$. The number noted in the figure was the contribution

604 ratio of the corresponding soil layers (0–20, 20–40, 40–100, 100–200 cm).